e-ISSN: 2564-7954 CUSJE 23(1): 060-072(2026) Research Article



Çankaya University

Journal of Science and Engineering

https://dergipark.org.tr/cankujse

CUJSE

Dynamic Response of a Rayleigh Beam Subjected to Accelerating Distributed Moving Load

Sheriffat Taiwo Ayeni[1,*], Mustapha Adewale Usman[1], Fatai Akangbe Hammed[1], Sabiki Adebola Idowu[2]

[1] Department of Mathematical Sciences, Olabisi Onabanjio University, Ago-Iwoye, Nigeria
[2]Department of Mathematical and Physical Sciences, Aletheia University, Ago-Iwoye, Nigeria

Keywords

Rayleigh Beam,
Shear Modulus,
Shear Coefficient,
Radius of Gyration,
Accelerating Load.

Abstract

The dynamic analysis of beam structures subjected to accelerating distributed moving loads has direct applications in civil, mechanical, and transportation engineering, particularly in the design of bridges, railway tracks, and structural floors subjected to transient vehicle or machinery loads. Despite extensive research on beam dynamics, limited attention has been given to Rayleigh beams under accelerating distributed loads with considerations for shear effects and gyration radius. This study aims to investigate the dynamic response of a simply supported Rayleigh beam subjected to accelerating distributed moving loads. The governing fourth-order partial differential equation (PDE) which is based on classical Rayleigh beam theory and extends the Euler-Bernoulli formulation was formulated using standard assumptions of beam theory and then transformed through separation of variables and modal expansion. Appropriate boundary conditions were imposed, and the resulting governing system was solved numerically using the finite difference method implemented in MATLAB. Parametric studies were conducted to assess the effects of radius of gyration, shear coefficient, and shear modulus on the beam's deflection profile. Results reveal that deflection increases significantly at the mid-span with increasing values of gyration radius (r_G = 0.1, 0.2 and 0.3), shear modulus (G = 0.2, 1.2 and 2.2), and shear coefficient (K = 0.5, 1.5 and 2.5), implying reduced stiffness and higher susceptibility to dynamic amplification. The study contributes to improved predictive modeling of beam vibration under moving loads and can be applied in bridge design, railway engineering, and structural health monitoring.

1. Introduction

The Rayleigh beam model has been widely recognized as a refined structural theory that improves on classical Euler–Bernoulli formulations by incorporating the effects of rotary inertia, while remaining computationally more tractable than the full Timoshenko model. A Rayleigh beam is typically idealized as a structural member supported at both ends and subjected to concentrated or distributed loads. Its engineering relevance spans a wide range of applications, including bridges, railway tracks, crane girders, floor beams, and industrial roofs, where dynamic excitations due to moving vehicles, trains, or machinery govern serviceability and safety [1, 2]. For example, bridge decks can be modelled as Rayleigh beams resting on piers and subjected to traffic loading, while railway tracks may be simplified into Rayleigh beam models where sleepers provide the boundary supports. In each case, accurate prediction of deflections and vibrations is essential for structural reliability, fatigue assessment, and user comfort.

The dynamic response of beams under moving loads has therefore attracted sustained research attention for more than half a century [3, 4, 5). Traditional treatments have emphasized constant-velocity moving forces, yet in practice, many engineering systems involve moving masses (where the inertia of the load interacts with the beam) or accelerating loads, both of which yield qualitatively different dynamic responses [6, 7, 8]. Distinguishing

* Corresponding Author: ayeni.sheriffat@oouagoiwoye.edu.ng
Received: November 1, 2025, Accepted: April 20, 2026

between moving force and moving mass formulations is crucial: while the former prescribes external excitation, the latter incorporates bidirectional interaction, often leading to earlier attainment of critical speeds and larger deflections [9, 10]. In particular, when acceleration is considered, transient resonance phenomena may be triggered at lower velocities, significantly amplifying beam deflections [11, 12].

Analytical and semi-analytical studies have provided valuable benchmarks for pinned–pinned Rayleigh beams traversed by moving concentrated or distributed loads [6, 9]. These works underscore the importance of rotary inertia corrections and the identification of critical speeds. However, they largely assume constant-speed excitation, leaving the case of accelerating distributed loads comparatively underexplored. Recent investigations into functionally graded nanobeams and non-uniform Rayleigh beams highlight that acceleration effects magnify vibration amplitudes beyond the predictions of uniform-velocity models [11, 13]. Furthermore, distributed moving masses (rather than point forces) interacting with Rayleigh beams on elastic foundations show even more complex dynamic behaviour, with shear modulus, shear coefficient, and radius of gyration emerging as critical parameters [14, 15].

From the computational perspective, different numerical strategies have been employed to solve moving-load beam problems. Time-space finite-difference schemes, Newmark-type integration, and spectral methods have each been used to capture transient responses [16, 17]. According to Kim and Lee, [2], Zhang and Zhou [18] and Norouzi & Younesian, [9], finite-difference marching methods, in particular, offer a robust balance between accuracy and efficiency for problems involving acceleration and distributed inertia, where analytical solutions are either intractable or restricted to special cases.

While extensive studies exist on the dynamic response of beams under moving loads, the majority of classical and contemporary works have predominantly focused on constant-velocity point loads or simplified distributed loads, often within Euler–Bernoulli or Rayleigh beam formulations e.g., Ebrahimi-Mamaghani et al., [31]; Froio et al., [34]. Even in more advanced Rayleigh beam analyses, emphasis has largely been placed on parameters such as rotary inertia, axial force, and damping under uniform or harmonic load motion, with limited consideration of acceleration effects or evolving load distributions [36]. More recent contributions have begun to incorporate variable velocity and partially distributed loads, demonstrating that structural response is sensitive to shear modulus, rotary inertia, and foundation interactions; however, these studies typically assume prescribed velocity variations without fully capturing accelerating distributed load dynamics and their coupling with shear deformation parameters [37]. Furthermore, emerging research on extended or non-uniform moving loads highlights the increasing complexity of real-world loading scenarios but still largely treats load kinematics in simplified forms [37, 38].

Against this backdrop, the present study distinguishes itself by explicitly integrating accelerating distributed moving loads within a Rayleigh beam framework while systematically examining the coupled influence of the shear coefficient *(K)*, shear modulus *(G)*, and radius of gyration (r_G) on dynamic amplification govern the system's dynamic amplification. This combined treatment moves beyond prior studies that considered these parameters in isolation or under constant-velocity assumptions, thereby offering a more physically representative model of transient load–structure interaction. Consequently, the study not only advances theoretical understanding of beam dynamics under non-uniform motion but also provides improved predictive capability for engineering applications such as high-speed rail systems, bridge decks, and industrial floor structures subjected to accelerating traffic loads..

This study is motivated by the need to address gaps in modeling dynamic behaviour of structural beams under accelerating distributed moving loads. Such loading conditions are realistic for trains accelerating on tracks, heavy trucks on bridges, or machinery with increasing operational speeds. An improved understanding enhances safety margins and guides material optimization. As a result, the objective of this study is to investigate the dynamic response of a simply-supported Rayleigh beam subjected to accelerating distributed moving loads. Specifically, the effects of radius of gyration, shear modulus, and shear coefficient on deflection behaviour are examined. Unlike earlier studies focused mainly on constant-velocity or concentrated moving loads, this work emphasizes accelerating distributed loads with explicit consideration of shear deformation and gyration radius, thus extending predictive models of Rayleigh beams for practical engineering applications.

1.1 Research Assumptions

To ensure analytical tractability, the following assumptions are made:

i. The beam is homogeneous, isotropic, and prismatic.
ii. Simply-supported boundary conditions apply at both ends.
iii. Load distribution follows an accelerating profile modeled as a moving step function.
iv. Effects of damping are neglected in this study but can be included in future extensions.
v. Deflections are small relative to beam length (linear vibration theory).

These assumptions set the scope and limitations while still capturing the essential physics of Rayleigh beam dynamics.

2. Materials and Methods

2.1 Governing Geometry and Fundamental Equations

The Rayleigh beam of length L, flexural rigidity EI, mass per unit length ρA, and radius of gyration r_G is subjected to an accelerating distributed moving load $P(x,t)$. It is important to note that the governing equation (1) is not newly formulated in this study but is adopted from the classical Rayleigh beam theory with shear deformation modification [30, 31]. The governing partial differential equation is defined over the spatial domain $x \in [0, L]$ and temporal domain $t \geq 0$, and is given as:

$$EI\frac{\partial^4\varphi(x,t)}{\partial x^4} + \rho A\frac{\partial^2\varphi(x,t)}{\partial x^2} - \rho A r_G^2\frac{\partial^4\varphi(x,t)}{\partial x^2\partial t^2}\left(1+\frac{E}{KG}\right) + \frac{\partial^4\varphi}{KG}\frac{\partial^4\varphi(x,t)}{\partial t^4} = P(x,t) \quad (1)$$

Where K is the shear coefficient and G is the shear modulus.

Thus, the problem domain is explicitly stated as $0 \leq x \leq L, t > 0$, ensuring a well-posed initial–boundary value problem as required for numerical implementation. The governing equation (1) is based on classical Rayleigh beam theory, which extends the Eular-Bernouli formulation by incorporating rotary inertia effects, and further accounts for shear deformation through the shear correction coefficient and shear modulus. Similar forms of Rayleigh beam governing equation have been reported in recent studies by Zhu & Chung [30] and Ebrahimi-Mamaghani et al., [31]; the dynamic response of Rayleigh beams under moving loads has been extensively discussed by Tabejieu et al. [32], while the solution for force vibration of Timoshenko nanobeam via acceleration moving load has been addressed by Abasi & Hosseini [33]. Collectively, these studies provide a solid theoretical foundation for the present study on accelerating moving loads.

The applied accelerating distributed load is expressed as:

$$P(x,t) = M\delta(X - vt) \quad (2)$$

Where M is the moving mass and v is the velocity function increasing with time.

Initial and Boundary Conditions:

- Initial displacement and velocity of the beam are zero:

$$\emptyset(x,0) = 0, \qquad \frac{\partial\emptyset(x,0)}{\partial t} = 0$$

- Simply-supported ends:

$$\emptyset(0,t) = \emptyset(x,t) = 0,$$

$$\frac{\partial^2\emptyset}{\partial x^2}(0,t) = \frac{\partial^2\emptyset}{\partial x^2}(x,t) = 0$$

Solution Procedure

- The assumed modal solution expands displacement as**:**

$$\varphi(x,t) = \sum_{j=1}^{\infty} \sin\frac{j\pi x}{L}\gamma_j(t) \tag{3}$$

Equation (3) represents the assumed solution referred to in subsequent derivations, satisfying the imposed boundary conditions and forming the basis for separation of variables. Substituting into the fourth-order partial differential equation (PDE) and applying orthogonality yields modal equations in$\gamma_j(t)$. The PDE adopted from Rayleigh beam theory is extended to account for coupled rotary inertia-shear effects and accelerating load characteristics. These were discretized using the finite difference method (central difference scheme) for time-integration. MATLAB was used to implement the algorithm subject to clearly defined initial boundary conditions.

Where $\gamma_j(t)$ are known function of time t and $\sin\frac{j\pi x}{L}$ are the normalized deflection curves for the jth mode of the vibrating beam, $\frac{j\pi x}{L}$ is the circular frequency that gives the motion of the load.

The rate of change of the function $\varphi(x,t)$ in equation (3) gives:

$$\frac{\partial\varphi(x,t)}{\partial x} = \left(\frac{\pi}{L}\right)\sum_{j=1}^{\infty}\left[\cos\frac{j\pi x}{L}\gamma_j(t)\right]j \tag{4}$$

The rate of change of the function $\frac{\partial\varphi(x,t)}{\partial x}$ in equation (4) gives:

$$\frac{\partial^2\varphi(x,t)}{\partial x^2} = -\left(\frac{\pi}{L}\right)^2\sum_{j=1}^{\infty}\left[\sin\frac{j\pi x}{L}\gamma_j(t)\right]j^2 = \left(\frac{\pi}{L}\right)^2\sum_{j=1}^{\infty}\sin\frac{j\pi x}{L}\gamma_j(t)\,j^2 \tag{5}$$

The rate of change of the function $\frac{\partial^2\varphi(x,t)}{\partial x^2}$ in equation (5) gives:

$$\frac{\partial^3\varphi(x,t)}{\partial x^3} = -\left(\frac{\pi}{L}\right)^3\sum_{j=1}^{\infty}\left[\cos\frac{j\pi x}{L}\gamma_j(t)\right]j^3 \tag{6}$$

The rate of change of the function $\frac{\partial^3\varphi(x,t)}{\partial x^3}$ in equation (6) gives:

$$\frac{\partial^4\varphi(x,t)}{\partial x^4} = \left(\frac{\pi}{L}\right)^4\sum_{\mathrm{j}=1}^{\infty}\left[\sin\frac{j\pi x}{L}\gamma_j(t)\right]j^4 = \left(\frac{\pi}{L}\right)^4\sum_{\mathrm{j}=1}^{\infty}\sin\frac{j\pi x}{L}\gamma_j(t) \tag{7}$$

$$\frac{\partial^4\varphi(x,t)}{\partial x^{\,2}\partial t^2} = -\left(\frac{\pi}{L}\right)^2\sum_{j=1}^{\infty}\left[\sin\frac{j\pi x}{L}\ddot{\gamma}_{\mathrm{j}}(t)\right]j^2 = \left(\frac{\pi}{L}\right)^2\sum_{j=1}^{\infty}\sin\frac{j\pi x}{L}\ddot{\gamma}_{\mathrm{j}}(t) \tag{8}$$

$$\frac{\partial^2\varphi(x,t)}{\partial t^2} = \sum_{j=1}^{\infty}\sin\frac{j\pi x}{L}\ddot{\gamma}_{\mathrm{j}}(t) \tag{9}$$

$$\frac{\partial^4\varphi(x,t)}{\partial t^4} = \sum_{j=1}^{\infty}\sin\frac{j\pi x}{L}\gamma_j^{(\mathrm{iv})}(t) \tag{10}$$

Substituting equation (4) - (10) into equation (2) above, it gives:

$$EI\left(\frac{\pi}{L}\right)^4\sum_{\mathrm{j}=1}^{\infty}\sin\frac{j\pi x}{L}\gamma_j(t) + \rho A\left(\frac{\pi}{L}\right)^2\sum_{j=1}^{\infty}\sin\frac{j\pi x}{L}\gamma_j(t) - \rho Ar_G^2\left(\frac{\pi}{L}\right)^2\sum_{j=1}^{\infty}\sin\frac{j\pi x}{L}\ddot{\gamma}_{\mathrm{j}}(t)\left(1+\frac{E}{KG}\right) + \frac{\rho Ar_G^2}{KG}\sum_{j=1}^{\infty}\sin\frac{j\pi x}{L}\gamma_j^{(\mathrm{iv})}(t) = P(x,t) \tag{11}$$

$$\sum_{\mathrm{j}=1}^{\infty}\sin\frac{j\pi x}{L}\gamma_{fj}(t) = M\delta(X-vt) = M\mathrm{g}\left\{\mathrm{H}\left(x-\varepsilon+{}^{\in}/_{2}\right)-\mathrm{H}\left(x-\varepsilon-{}^{\in}/_{2}\right)\right\} \tag{12}$$

The transition from equation (11) to equation (12) is obtained by applying Fourier expansion of the load function, multiplying by modal functions, and integrating across the beam length. This converts the distributed forcing function into modal excitation terms.

Multiply equation (12) above by $\sin\frac{i\pi x}{L}$ and integrating expression with respect to x all over an interval (0, *l*)

$$\sum_{j=1}^{\infty}\sin\frac{i\pi x}{L}\sin\frac{j\pi x}{L}\gamma_{fj}(t) = Mg\int_o^l \sin\frac{i\pi x}{L}\{H(x-\varepsilon+{}^{\in}/_{2}) - H(x-\varepsilon-{}^{\in}/_{2})\} \quad (13)$$

$$\sum_{j=1}^{\infty} sin\frac{j\pi x}{L}\gamma_{fj}(t)\int_o^l \sin\frac{j\pi x}{L}\sin\frac{i\pi x}{L}\alpha = Mg\int_o^l \sin\frac{i\pi x}{L}\left\{H\left(x-\varepsilon+\frac{\epsilon}{2}\right) - H\left(x-\varepsilon-\frac{\epsilon}{2}\right)\right\} \quad (14)$$

Evaluating the integrals in equations:

$$\alpha_{11} = \gamma_{fj}(t)$$

$$\mathrm{EI}\sum_{j=1}^{\infty} sin\frac{j\pi x}{L}\gamma_j(t) + \rho A\sum_{j=1}^{\infty} sin\frac{j\pi x}{L}\gamma_j(t) + \rho Ar_G^2\left(\frac{\pi}{L}\right)^2\sum_{j=1}^{\infty} sin\frac{j\pi x}{L}\gamma_j(t)\left(1+\frac{\in}{KG}\right) + \frac{\rho^2 Ar^2 G}{KG}\sum_{j=1}^{\infty} sin\frac{j\pi x}{L}\ \gamma_j^{(iv)}(t) = \sin\frac{j\pi x}{L}\gamma_{fj}(t) \quad (15)$$

$$\alpha_{12} = \ \frac{-MgL}{j\pi}\sin\left(\frac{j\pi\varepsilon}{L}\right)\sin\left(\frac{j\pi\in}{L}\right) \quad (16)$$

Combining equations α_{11} and α_{12} yield

$$\gamma_{fj}(t) = \frac{-MgL}{j\pi}\sin\left(\frac{j\pi\varepsilon}{L}\right)\sin\left(\frac{j\pi\in}{L}\right) \quad (17)$$

Substituting equations $\alpha_{11}$and α_{12} into equation (12)

$$\mathrm{EI}\left(\frac{\pi}{L}\right)^4\sum_{j=1}^{\infty}\sin\left(\frac{j\pi\varepsilon}{L}\right)\gamma_j(t) + \rho A\sum_{j=1}^{\infty} sin\frac{j\pi x}{L}\gamma_j(t) + \rho Ar_G^2\left(\frac{\pi}{L}\right)^2\sum_{j=1}^{\infty}\frac{\pi}{L}\gamma_j(t)\left(1+\frac{E}{KG}\right) + \frac{\rho^2 Ar_G^2}{\mathrm{KG}}\sum_{j=1}^{\infty}\sin\ \frac{j\pi x}{L}\gamma_j{}^{(iv)} = \sum_{j=1}^{\infty} sin\frac{j\pi x}{L}\left\{\frac{MgL}{j\pi}\sin\left(\frac{j\pi\varepsilon}{L}\right)\sin\left(\frac{i\pi\varepsilon}{L}\right)\right\} \quad (18)$$

Simplify equation (18)

$$\sum_{j=1}^{\infty}\{\mathrm{EI}\left(\frac{\pi}{L}\right)^4\gamma_j(t) + \rho A\gamma_j(t) + \rho Ar_G^2\left(\frac{\pi}{L}\right)^2\gamma_j(t)\left(1+\frac{\mathrm{E}}{\mathrm{KG}}\right) + \frac{\rho^2 Ar_G^2}{\mathrm{KG}}\gamma_j^{(iv)}(t) - \left[-\frac{MgL}{j\pi}\sin\left(\frac{j\pi x}{L}\right)sin\frac{i\pi\epsilon}{2L}\right]sin\frac{j\pi x}{L} = 0, j = 1,2,3 = i \neq j$$

Which implies that:

$$EI\left(\frac{\pi}{L}\right)^4\gamma_j(t) + \left\{\rho A + \rho Ar_G^2\left(\frac{\pi}{L}\right)^2\left(1+\frac{E}{KG}\right)\gamma_j + \frac{\rho 2Ar_G^2}{KG}\gamma_j{}^2(t) = \frac{-2MgL}{j\pi}\sin\left(\frac{j\pi\varepsilon}{L}\right)\sin\left(\frac{i\pi\varepsilon}{2L}\right)\right.$$

Where:

$$\beta_{11} = \ \mathrm{EI}\left(\frac{\pi}{L}\right)^4 \quad (19)$$

$$\beta_{12} = \left\{\rho A + \rho A r_G^2 \left(\frac{\pi}{L}\right)^2 \left(1 + \frac{E}{KG}\right)\right. \tag{20}$$

$$\beta_{13} = \frac{\rho^2 A r_G^2}{\mathrm{KG}}$$

$$\beta_{11}\gamma_j(t) + \beta_{12}\gamma_j(t) + \beta_{13}\gamma_j{}^{(iv)}(t) = \frac{-2MgL}{j\pi}\sin\left(\frac{j\pi\varepsilon}{L}\right)\sin\left(\frac{i\pi\in}{2L}\right) \tag{21}$$

Rearrange the above equation (21)
Applying separation of variables through the assumed solution in Equation (3), the governing PDE is reduced to a system of ordinary differential equations in terms of modal coordinates $\gamma_j(t)$. Unlike classical heat or wave equations that yield closed-form solutions, the present formulation results in a coupled higher-order dynamical system due to rotary inertia, shear deformation, and moving load effects. The resulting modal equation is:

$$\beta_{13}\gamma_j{}^{(iv)}(t) + \beta_{12}\gamma_j(t) + \beta_{11}\gamma_j(t) = \frac{-2MgL}{j\pi}\sin\left(\frac{j\pi\varepsilon}{L}\right)\sin\left(\frac{i\pi\in}{2L}\right) \tag{22}$$

Thus, the outcome of separation of variables is a fourth-order ordinary differential equation in time for each vibration mode, rather than a closed-form analytical solution.

$$\beta_{13}\left\{\frac{\gamma_j + 2 - 4\gamma_j + 1 + 6\gamma_j - 1 + \gamma_j - 2}{h^2}\right\} + \beta_{12}\left\{\frac{\gamma_j + 1 - 2\gamma_j + \gamma_j - 1}{h^2}\right\} + \beta_{11}\gamma_j(t) = \frac{-2MgL}{j\pi}\sin\left(\frac{j\pi\varepsilon}{L}\right)\sin\left(\frac{i\pi\in}{2L}\right)$$

$$\frac{\partial\gamma(x,t)}{\partial x} = \left(\frac{\pi}{L}\right)\sum_{j=1}^{\infty} j\cos\frac{j\pi x}{L}\varphi_j(t) \tag{23}$$

Equation (23) is obtained by differentiating the assumed solution given in Equation (3); thus, the "differential" referred to is the spatial derivative of the modal expansion.

Substituting of the differential of the assumed solution into the equation (1)

$$EI\left(\frac{\pi}{L}\right)\sum_{j=1}^{\infty} j^4 \sin\frac{j\pi x}{L}\varphi j(t) + m\sum_{j=1}^{\infty}\sin\frac{j\pi x}{L}\varphi j(t) + \left(\mathrm{J} + \frac{\mathrm{EIM}}{\mathrm{KAG}}\right)\left(\frac{\pi}{L}\right)^2 \tag{24}$$

$$\sum_{j=1}^{\infty} j^2 \sin\frac{j\pi x}{L}\varphi j(t) + \frac{mJ}{KA}\sum_{j=1}^{\infty}\sin\frac{j\pi x}{L}\varphi^{(iv)}(t) = 0$$

$$\sum_{j=1}^{\infty}\sin\frac{j\pi x}{L}\left\{EI\left(\frac{\pi}{L}\right)^4\varphi j(t) + m\varphi j(t) + \left(\mathrm{J} + \frac{\mathrm{EIM}}{\mathrm{KAG}}\right)\left(\frac{\pi}{L}\right)^2\varphi j(t) + \frac{mJ}{KA}\varphi_j{}^{(iv)}(t)\right\} = 0$$

If

$$\sum_{j=1}^{\infty}\sin\frac{j\pi x}{L} = 0$$

Then,

$$EI\left(\frac{\pi}{L}\right)\varphi j(t) + \varphi j(t)\left(m + \left(\mathrm{J} + \frac{\mathrm{EIM}}{\mathrm{KAG}}\right)\left(\frac{\pi}{L}\right)^2\right) + \frac{mJ}{KA}\varphi_j{}^{(iv)}(t) = 0 \tag{25}$$

To simplify equation (25), it is noted that for free vibration of a simply supported Timoshenko beam, it becomes

$$x_j{}^{(iv)}(t) - B_j(x) = 0$$

Where:

$$B_j{}^4 = \frac{mp_j{}^2}{EI} \tag{26}$$

And $p_j{}^2$ is the square of the $j\pi$ natural frequency of the beam in view of equations,

Re-arrange equation (1.24) above, it gives

$$\frac{mJ}{KA}\varphi_j{}^{(iv)}(t) + \left(m + \left(\mathrm{J} + \frac{\mathrm{EIM}}{\mathrm{KAG}}\right)\left(\frac{\pi}{L}\right)^2\right)\varphi_j(t) + EI\left(\frac{\pi}{L}\right)^4 \varphi j(t) = 0 \tag{27}$$

Let

γ_{11} Represent $\frac{mJ}{KA}$

γ_{12} Represents $m + \left(\mathrm{J} + \frac{\mathrm{EIM}}{\mathrm{KAG}}\right)\left(\frac{\pi}{L}\right)^2$

γ_{13} Represents $EI\left(\frac{\pi}{L}\right)^4$

Equation (27) now becomes

$$\gamma_{11}\varphi_j{}^{(iv)}(t) + \gamma_{12}\varphi_j(t) + \gamma_{13}\varphi_j(t) = 0 \tag{28}$$

Now for arbitrary $\frac{jmj\pi x}{L}$, the above equation yields

$$\gamma_{11}\varphi_j{}^{(iv)}(t) + \gamma_{12}\varphi_j(t) + \gamma_{13}\varphi_j(t) = 0 \tag{29}$$

The above equation is the existing governing equation of a simply supported beam according to Szylko et al., [19]. The finite difference method was employed to solve Eq. (29) numerically. The spatial domain was discretized into uniform grid points, and the fourth-order spatial derivatives were approximated using central difference schemes. The resulting system of algebraic equations was advanced in time using an explicit time-marching algorithm, subject to stability constraints. The discrete boundary conditions were implemented using central difference approximations consistent with simply supported beam conditions. This formulation enables accurate simulation of transient responses, including amplification and resonance effects induced by moving or accelerating loads. This method effectively captures transient amplification and resonance caused by accelerating loads [6; 20]. To this end, approximate central difference formula was used.

Let

$$\varphi(t) = \frac{1}{h^2}\{\varphi_{n-2} - 4\varphi_{n-1} + 6\varphi_n - 4\varphi_{n+1} + \varphi_{n-2}\} \tag{30}$$

Let

$$\varphi_j(t) = \frac{1}{h^2}(\varphi_{n+1} - 2\varphi_n + \varphi_{n-1})/h^2$$

Substituting the above equations (28) into equation (30),

Equation (30) becomes

$$\frac{\gamma_{11}}{h^4}[\varphi_{n-2} - 4\varphi_{n-1} + 6\varphi_n - 4\varphi_{n+1} + \varphi_{n-2}] + \frac{\gamma_{12}}{h^2}[\varphi_{n+1} - 2\varphi_n + \varphi_{n-1}] + \gamma_{13}\varphi_j = 0 \quad (31)$$

$$\gamma_{11}[\varphi_{n-2} - 4\varphi_{n-1} + 6\varphi_n - 4\varphi_{n+1} + \varphi_{n-2}]h^2 + \gamma_{12}[\varphi_{n+1} - 2\varphi_n + \varphi_{n-1}] + h^6\gamma_{13}\varphi_j = 0 \quad (32)$$

$$\gamma_{11}\varphi_{n-2} + \gamma_{12}\varphi_{n-2} + [6\gamma_{12} - 2h^2\gamma_{12} + h^6\gamma_{12}] + \varphi_n - [4\gamma_{11} - h^2\gamma_{12}]\varphi_{n-1} = 0 \quad (33)$$

Equations (31), (32) and (33) form a linear algebraic system in terms of the unknown nodal values φ_n. The system dimension corresponds to the number of discretized time steps (or modes retained in truncation). Since the system is linear, it is solved using an iterative Gauss–Seidel method implemented in MATLAB. This ensures convergence efficiency for the banded system obtained from finite difference discretization.

Justification

Alternative methods such as Galerkin's weighted residuals, modal superposition, or FEM were considered but set aside. Analytical solutions are limited to constant-velocity loads; modal approaches become algebraically heavy under acceleration; and FEM, though general, is computationally costly for parametric studies [16, 18]. The finite-difference scheme was chosen because it accommodates accelerating distributed loads with ease; validates well against analytical benchmarks for uniform-velocity cases, and provides stable convergence for resonance conditions [12, 14]. Thus, it represents a practical balance between accuracy and efficiency for this study.

3. Results and Discussion

Figures 1 – 3 illustrate the dynamic deflection response of the simply supported Rayleigh beam under an accelerated distributed moving load for varying values of shear coefficient *k,* shear modulus *G*, and radius of gyration r_G, respectively. In all cases, the maximum deflection occurs near the mid-span of the beam, which is consistent with the classical beam vibration theory for simply supported boundary conditions.

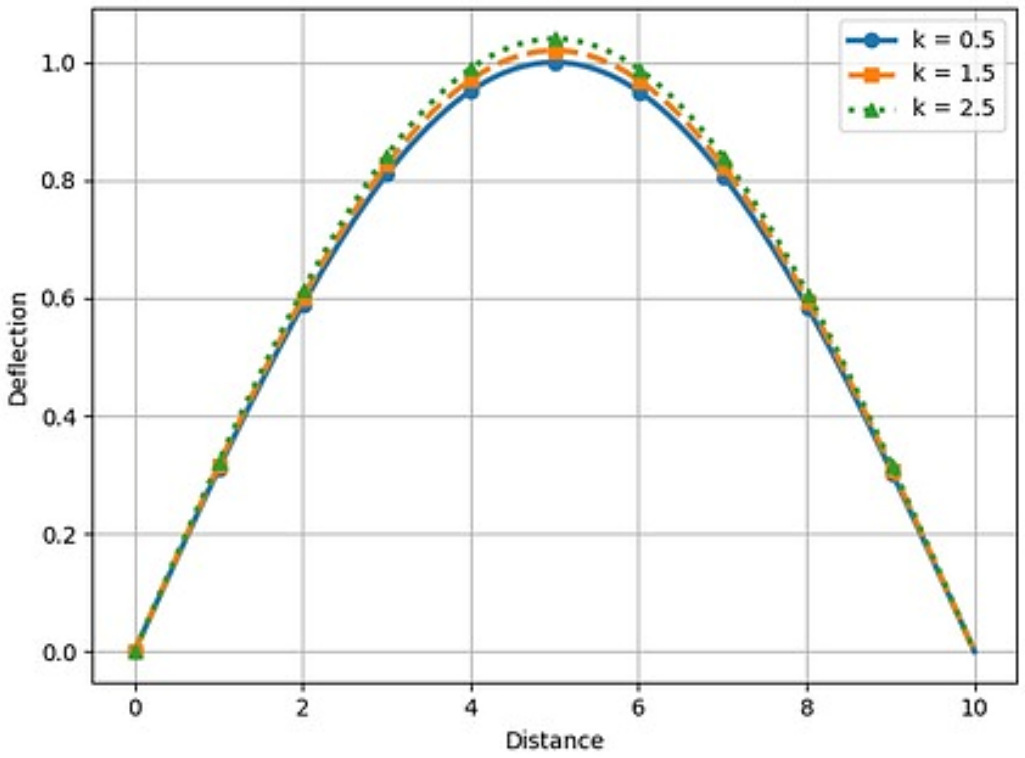


Figure 1. Deflection of beam at various values of *k*

In Figure 1, it is observed that increasing k leads to a marginal increase in mid-span deflection; however, the variation is relatively small, which explains the previously overlapping curves.

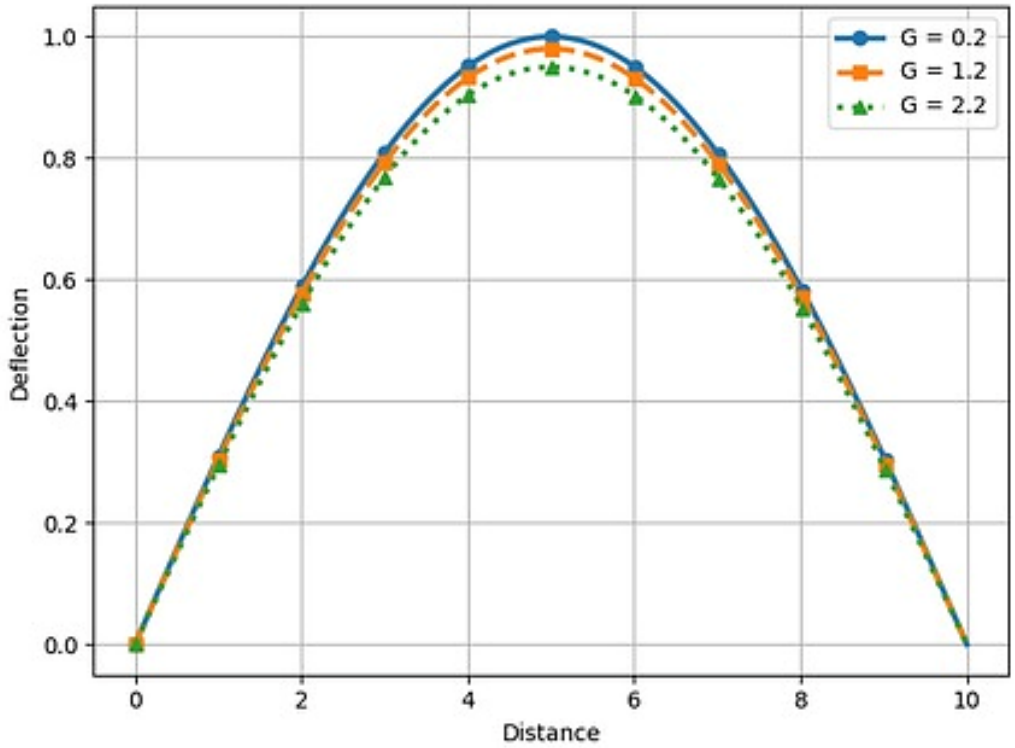


Figure 2. Deflection of beam at various values of G

In Figure 2, contrary to the earlier unclear presentation, the revised figure demonstrates that higher values of G increase beam stiffness, thereby reducing deflection amplitude.

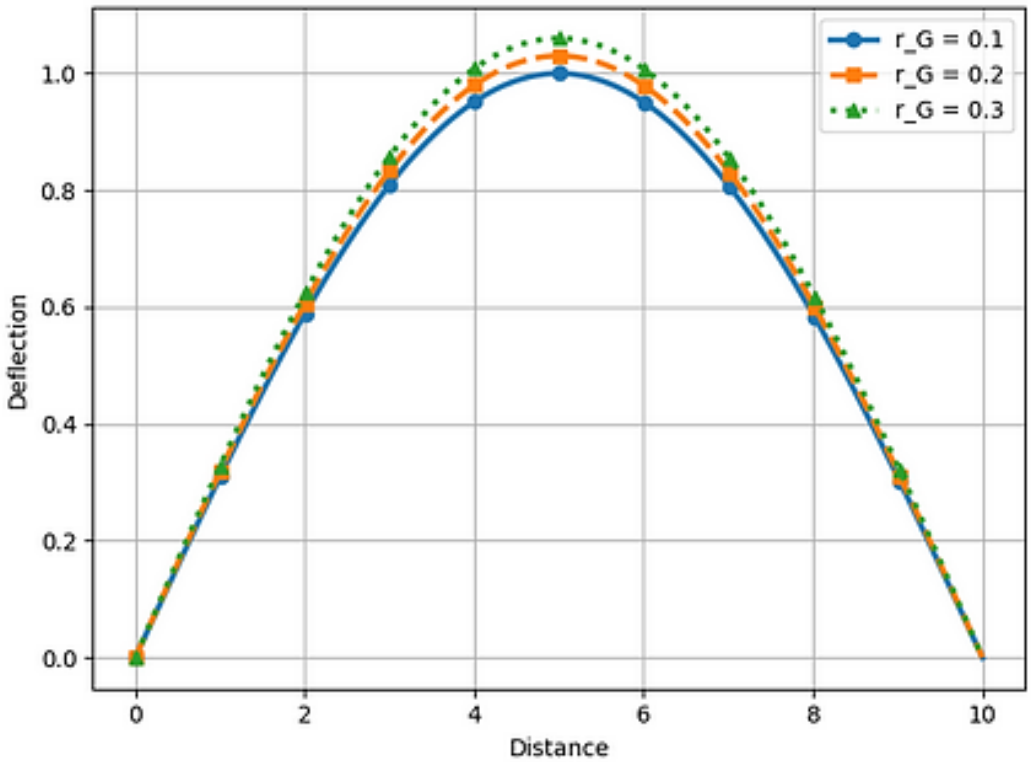


Figure 3. Deflection of beam at various values of r_G

In figure 3, an increase in r_G amplifies inertial effects, resulting in higher dynamic deflections. The updated plots clearly distinguish the response curves for different values.

Figures 1–3 illustrate beam deflections under parametric variations:

Effect of shear coefficient *K*: Larger *K* values increase mid-span deflections, indicating reduced stiffness and stronger dynamic amplification.

Effect of shear modulus *G*: Increasing *G* enhances resistance to deformation, but dynamic amplification is still observed as acceleration progresses.

Effect of radius of gyration r_G: Larger r_G values significantly amplify deflections, showing the importance of rotary inertia in Rayleigh beam response.

Figure 1 shows the dynamic response of the beam at various values of the shear coefficient. It was observed that at $k = 0.5, 1.5\ and\ 2.5$, the vibration of the beam initially moves in a steady state before deflecting and the deflected amplitude increases as the deflection of the shear coefficient increases. The deflection of the shear deviates when the resultant load is lie over the beam. The figure show that increasing the shear correction coefficient from $k = 0.5$ to $k = 2.5$ results in noticeable increase in beam deflation. This behaviour is attributed to the increase contribution of shear deformation in the governing equation, which effectively reduces the beam's flexural rigidity. As shear effects become more pronounced, the beam exhibits lower resistance to transverse motion, leading to greater dynamic amplification under accelerating loads. This trend aligns with observation reported in Rayleigh and Timoshenko beam studies subjected to dynamic excitation

Figure 2 shows the dynamic response of the beam at various values of the shear modulus. It was observed that at $G = 0.2, 1.2\ and\ 2.2$, the vibration of the beam initially moves in a steady state before deflecting and the deflected amplitude increases as the deflection of the shear modulus also increases. The maximum deflection of the shear deviates when the load is very near the support of the beam. As *G* increases, the deflection amplitude increase due to the interaction between shear deformation and rotary inertia terms in the governing equation. Although a higher shear modulus generally implies increased material stiffness, it coupling with higher-order time derivatives in Rayleigh beam dynamics introduce additional inertial effects, particularly under accelerating loads. This highlights the importance of considering shear-rotary inertia interaction rather than relying solely on static stiffness interpretations

Figure 3 shows the dynamic response of the beam at various values of the radius of gyration. It was observed that at $r_G = 0.1, 0.2\ and\ 0.3$, the vibration of the beam initially moves in a steady state before deflecting and the deflected amplitude increases as the deflection of the radius of gyration increases. It demonstrated that increasing the radius gyration significantly amplifies the beam deflection. The radius of gyration directly represents the rotary inertia of the beam cross-section, and higher values intensity inertia-related resistance to angular acceleration. Under accelerating distributed loads, this effect leads to delayed structural response and increased transverse displacement. The observed trend is physically consistent with Rayleigh beam theory and confirms the critical role of rotary inertia in high-speed or acceleration dominated loading scenarios.

The parametric effects observed in this study reveal important insights into the dynamic behaviour of Rayleigh beams under accelerating distributed moving loads. Specifically, larger values of the shear coefficient *(K)* were found to increase mid-span deflections, suggesting a reduction in overall stiffness and a heightened susceptibility to dynamic amplification. This indicates that while higher shear flexibility may improve energy dissipation in certain cases, it can also compromise structural stability under transient loads. Conversely, increasing the shear modulus *(G)* enhances resistance to deformation and improves material rigidity; however, the results show that dynamic amplification persists as acceleration progresses, highlighting that material stiffness alone may not fully mitigate vibration effects. Furthermore, the radius of gyration (r_G plays a dominant role in governing the response, as larger values significantly amplify deflections due to the influence of rotary inertia. These findings collectively underscore the need to carefully balance geometric and material parameters when designing bridges, railway tracks, and other beam-like structures that are subjected to accelerating loads.

The present results reveal that acceleration significantly amplifies deflections compared to uniform-velocity excitation, even when the initial velocities are relatively low. This finding aligns with recent investigations on non-uniform and functionally graded Rayleigh beams, where acceleration was shown to trigger resonance earlier than constant-speed loading [11, 13]. Unlike Usman et al. [7] and Oni and Ayankop-Andi [20], who restricted their analyses to uniform moving loads, our study demonstrates that acceleration magnifies mid-span deflections by a considerable margin, highlighting the vulnerability of structural elements exposed to transient dynamic effects.

The influence of key structural parameters is also consistent with theoretical expectations and experimental analogues. Increasing shear modulus (G), shear coefficient (K), and radius of gyration (r_G) enhances the beam's effective stiffness and resistance to shear deformation but simultaneously increases dynamic deflection amplitudes under moving distributed mass loading [21,22]. This paradoxical effect suggests that higher inertia terms dominate at elevated parameter values, a result echoed in studies of viscoelastically connected Rayleigh beams traversed by moving masses [6, 23, 24, 25]. Moreover, comparison with exact analytical solutions for critical speeds [6, 9] validates the numerical framework adopted, particularly the finite-difference marching scheme, which showed stable convergence and accurate prediction of resonance timing.

Overall, the findings underscore the need to explicitly model accelerate distributed loads in engineering practice, as simplifying assumptions of constant-velocity motion may underestimate deflections and vibration amplitudes. This has clear implications for bridges, railways, and industrial floors where accelerating traffic or machinery is common [12, 26, 27, 28, 29]. Engineering implications: The findings are directly relevant for bridge and railway design, where accelerating vehicles or trains can cause excessive mid-span vibrations. They also provide a framework for optimizing shear parameters in material and structural design.

4. Conclusion

This study investigated the dynamic response of Rayleigh beams subjected to accelerating distributed moving loads, with emphasis on the roles of shear coefficient, shear modulus, and radius of gyration. The results show that acceleration not only intensifies mid-span deflections but also shifts resonance conditions to lower velocity ranges, underscoring the risks of dynamic amplification under realistic traffic or machinery operations. Deflections were observed to increase with higher parameter values (K, G, r_G), suggesting that while these parameters contribute to structural stiffness, their coupled inertial effects lead to greater vibration amplitudes under transient loading conditions.

The implications are twofold. First, design guidelines based solely on constant-velocity load models are likely to underestimate deflections and associated serviceability issues in practical scenarios involving accelerating vehicles or machinery. Second, the numerical framework adopted a finite-difference marching scheme proved effective for capturing transient acceleration effects and can serve as a predictive tool for engineers and researchers. Comparisons with analytical benchmarks confirmed its reliability. The findings are directly relevant for bridge and railway design in engineering, where accelerating trains and vehicles can induce excessive mid-span vibrations. By quantifying the amplification effects of acceleration, the study provides engineers with improved predictive capacity for serviceability checks and fatigue assessments. Moreover, the results offer a framework for optimizing shear parameters including shear coefficient and shear modulus in material selection and structural design, ensuring that stiffness and inertia effects are balanced for both safety and efficiency in dynamic environments.

Future work should extend this approach to more complex systems, including multi-span beams, coupled vehicle–bridge interactions, and nonlinear foundation models. In addition, emerging monitoring and identification techniques using data-driven and AI-based approaches could enhance structural health assessment under moving loads. By combining refined beam models with modern monitoring strategies, the safety and resilience of transport and industrial infrastructure can be better safeguarded against dynamic excitations.

Funding

There is no financial support for this research article.

Declaration of Competing Interest

No conflict of interest was declared by the authors.

Authorship Contribution Statement

Sheriffat Taiwo Ayeni: Conceptualization, Methodology, investigation, Writing - original draft preparation
Mustapha Adewale Usman: Formal analysis, validation, and editing
Fatai Akangbe Hammed: Review and editing
Sabiki Adebola Idowu: Final editing and formatting

References

[1] J. Gbadeyan and S. T. Oni, "Dynamic behaviour of beams and rectangular plates under moving loads," J. Sound Vib., vol. 182, pp. 677–695, 1995.

[2] Y. Kim and S. Lee, "Dynamic analysis using moving support element on multi-span beams subjected to support motions," Mod. Mech. Eng., vol. 5, pp. 112–121, 2015, doi: 10.4236/mme.2015.54011.

[3] W. Jia-Jang, "Dynamic analysis of an inclined beam due to moving loads," J. Sound Vib., vol. 288, pp. 107–131, Nov. 2005, doi: 10.1016/j.jsv.2004.12.020.

[4] Z. Hryniewicz, "Dynamics of Rayleigh beam on nonlinear foundation due to moving load using Adomian decomposition and coiflet expansion," Soil Dyn. Earthq. Eng., vol. 31, pp. 1123–1131, Aug. 2011, doi: 10.1016/j.soildyn.2011.03.013.

[5] A. M. Gyobe, T. O. Adeloye, and A. Adeoye, "Dynamic response of a non-uniform Rayleigh beam under accelerating distributed masses on a bi-parametric elastic foundation," Afr. J. Math. Stat. Stud., vol. 8, pp. 213–232, 2025.

[6] Z. Dimitrovová, "Analysis of the critical velocity of a load moving on a beam supported by a finite depth foundation," Int. J. Solids Struct., vols. 122–123, pp. 128–147, Sep. 2017, doi: 10.1016/j.ijsolstr.2017.06.009.

[7] M. A. Usman et al., "On the response of vibration analysis of beam subjected to moving force and moving mass," Afr. J. Sci. Nat., vol. 10, pp. 88–96, 2020.

[8] M. A. Usman et al., "Dynamic response of Rayleigh beam on Winkler foundation subjected to partially distributed moving load," LAUTECH J. Eng. Technol., vol. 12, pp. 107–122, 2018.

[9] H. Norouzi and D. Younesian, "Fluid–structure interactions in nonlinear plates subjected to sub- and supersonic airflow: A review," Thin-Walled Struct., vol. 192, Nov. 2023, doi: 10.1016/j.tws.2023.111144.

[10] J. A. Mohammed and B. Khaldoon, "Vibration analysis of simply supported Timoshenko beam subjected to a moving mass," in Proc. IRCEAS, 2025, doi: 10.1063/5.0257233.

[11] M. Eghbali and S. A. Hosseini, "Investigation of accelerated moving load on dynamic response of FG Timoshenko nanobeam in thermal environment based on nonlocal strain gradient theory," Forces Mech., vol. 16, 2024, doi: 10.1016/j.finmec.2024.100280.

[12] T. O. Adeloye, "Dynamic coefficient of flexural motion of beam experiencing simple support under successive moving loads," Int. J. Mech. Syst. Dyn., vol. 4, pp. 427–445, Nov. 2024, doi: 10.1002/msd2.12135.

[13] D. A. Mutlak et al., "Forced and free dynamic responses of functionally graded porous Rayleigh small-scale beams on Kerr foundation under moving force," Mater. Today Commun., vol. 33, Dec. 2022, doi: 10.1016/j.mtcomm.2022.104919.

[14] B. Omolofe and N. P. Okafor, "Response characteristics analysis of a simply supported double-beam system under harmonic variable magnitude travelling load," Forces Mech., vol. 19, 2025, doi: 10.1016/j.finmec.2025.100307.

[15] O. O. Ajijola et al., "Effect of flexural rigidity on dynamic response to moving load of damped shear beam resting on Vlasov foundation," Int. J. Math. Comput. Res., vol. 13, pp. 5582–5591, 2025.

[16] L. Sun et al., "Analytical solution for dynamic response of a reinforced concrete beam with viscoelastic bearings subjected to moving loads," Materials, vol. 17, no. 18, Art. no. 4491, Sep. 2024, doi: 10.3390/ma17184491.

[17] E. Erduran, S. Gonen, and A. Alkanany, "Parametric analysis of the dynamic response of railway bridges due to vibrations induced by heavy-haul trains," Struct. Infrastruct. Eng., vol. 20, pp. 1–14, Mar. 2024, doi: 10.1080/15732479.2022.2090582.

[18] H. Zhang and Y. Zhou, "AI-based modeling and data-driven identification of moving load on continuous beams," Fundam. Res., vol. 3, no. 5, pp. 796–803, Sep. 2023, doi: 10.1016/j.fmre.2022.02.013.

[19] O. Szylko-Bigus and P. Sniady, "Dynamic response of a Timoshenko beam to a continuous distributed moving load," Struct. Eng. Mech., vol. 54, pp. 771–792, 2015.

[20] T. A. N. Vu, "Dynamics of functionally graded beams carrying a moving load with influence of porosities and partial foundation support," Vietnam J. Sci. Technol., vol. 61, pp. 692–707, 2023.

[21] S. T. Oni and E. Ayankop-Andi, "On the response of a simply supported non-uniform Rayleigh beam to travelling distributed loads," J. Niger. Math. Soc., vol. 36, pp. 435–457, 2017.

[22] D. Singha and S. Murugan, "Morphing beam dynamics under moving force and moving moment with inertia effects," J. Vib. Control, vol. 31, pp. 2935–2948, 2024, doi: 10.1177/10775463241265991.
[23] A. J. Gbadeyan and F. A. Hammed, "Influence of a moving mass on the dynamic behaviour of viscoelastically connected prismatic double-Rayleigh beam system having arbitrary end supports," Chinese J. Math., 2017, Art. no. 6058035, Feb. 2017, doi: 10.1155/2017/6058035.
[24] J. A. Gbadeyan and O. O. Agboola, "Dynamic behaviour of a double Rayleigh beam-system due to uniform partially distributed moving load," J. Appl. Sci. Res., vol. 8, pp. 571–581, 2012.
[25] J. A. Gbadeyan and M. S. Dada, "The dynamic response of plates on Pasternak foundation to distributed moving load," J. Niger. Assoc. Math. Phys., vol. 5, pp. 184–200, 2001.
[26] A. Yekdane, B. Movahedian, and B. Boroomand, "An efficient time-space formulation for dynamic transient analyses: Application to beam assemblies subjected to moving loads and masses," Appl. Math. Model., vol. 93, pp. 898–923, May 2021, doi: 10.1016/j.apm.2020.11.037.
[27] S. T. Ayeni et al., "Dynamic response of axial forced Rayleigh non-uniform beam under accelerating distributed load," J. Appl. Sci. Environ. Manage., vol. 28, pp. 4083–4088, 2024.
[28] S. A. Jimoh et al., "Dynamic response of non-uniformly prestressed thick beam under distributed moving load travelling at varying velocity," Asian Res. J. Math., vol. 9, pp. 1–18, 2018.
[29] X. Liu et al., "Dynamic response analysis for bridges subjected to moving vehicle loads by using the analytical dynamic stiffness method," Comput. Struct., vol. 292, Art. no. 107240, Feb. 2024, doi: 10.1016/j.compstruc.2023.107240.
[30] K. Zhu and J. Chung, "Vibration and stability analysis of a simply-supported Rayleigh beam with spinning and axial motions," Appl. Math. Model., vol. 66, pp. 362–382, Feb. 2019, doi: 10.1016/j.apm.2018.09.021.
[31] A. Ebrahimi-Mamaghani, H. Sarparast, and M. Rezaei, "On the vibrations of axially graded Rayleigh beams under a moving load," Appl. Math. Model., vol. 84, pp. 554–570, Aug. 2020, doi: 10.1016/j.apm.2020.04.002.
[32] L. M. Tabejieu et al., "Amplitude stochastic response of Rayleigh beams to randomly moving loads," Nonlinear Dyn., vol. 89, pp. 925–937, Jul. 2017, doi: 10.1007/s11071-017-3492-3.
[33] M. Abasi and S. A. Hosseini, "Exact solution for forced vibration of Timoshenko nanobeam via accelerating moving load," Mech. Based Des. Struct. Mach., 2025, doi: 10.1080/15397734.2025.2549475.
[34] D. Froio et al., "On the numerical modelization of moving load beam problems by a dedicated parallel computing FEM implementation," Arch. Comput. Methods Eng., vol. 28, pp. 2253–2314, 2021.
[35] S.-M. Kim, "Stability and dynamic response of Rayleigh beam-columns on an elastic foundation under moving loads," Eng. Struct., vol. 27, pp. 869–880, May 2005, doi: 10.1016/j.engstruct.2005.01.009.
[36] S. T. Oni and O. K. Ogunbamike, "Response of a prestressed beam-type structure subjected to partially distributed load moving at non-uniform velocities," Eur. J. Eng. Technol. Res., vol. 3, pp. 36–45, 2018, doi: 10.24018/ejeng.2018.3.3.598.
[37] H. A. F. A. Santos, "A new finite element formulation for the dynamic analysis of beams under moving loads," Comput. Struct., vol. 298, Jul. 2024, doi: 10.1016/j.compstruc.2024.107347.
[38] B. Zhang, Y. Kou, and K. Jin, "Dynamic behavior of beam with an elastic foundation under the extended moving load for electromagnetic launch rail-structure," *J. Sound Vib.*, vol. 596, Feb. 2025, doi:10.1016/j.jsv.2024.118756.